

The Improvement of the Powering Performance on the Japan Bulk Carrier (JBC) using Rudder Thrust Fin as a Post-Swirl Stator

Iwan Mustaffa Kamal, Md Salim Kamil, Yaseen Adnan Ahmed, Nur Aqilah Elias



Abstract: Post Swirl Stator (PSS), also known as the 'Energy Saving Device (ESD) Behind the Propeller' operates within the slip stream of the propeller. The aim of this project is to investigate the powering performance of a JAPAN Bulk Carrier (JBC) upon the installation of PSS. The prediction of resistance and propulsive factors were conducted using CFD simulation using SHIPFLOW CFD code. In order to find the optimised design of the ESD, three parameters were laid out and studied. The parameters are the left side fin length, right side fin length and the orientation of the fins. The aim of this study are to improvise the thrust fin design by changing the parameters to get the optimum powering performance result, and to quantify the powering performance of the JBC upon the installation of PSS in model and full scale. There were 27 different post-swirl stator configurations. All the 27 different configurations were compared in terms of its performance in model and full scale. All the 27 different configurations were simulated using full RANSE. The free surface of the water were modelled using panel method. A grid dependence study was conducted to determine the best grid cell resolution and it was chosen at a total of 7 millions cells. The bare hull resistance of the JBC were validated with available published experiment results. All the thrust fins were modelled using appendage setting in SHIPFLOW. The best thrust fins design were selected in judging its minimum drag, minimum thrust deduction fraction, minimum wake fraction, and the delivered power. It was found that the thrust fins design for case study #20 by CFD is the most optimised configuration in terms of its performance criteria as mentioned earlier. The thrust fins design was able to reduce delivered power to 6.012%. Thrust deduction was also reduced to 2.927%. Total efficiency was increased to 6.709%.

Index Terms: Post-Swirl Stator, Energy Saving Device, CFD.

I. INTRODUCTION

Recently there are demands from shipowners to have their modern fleets to be equipped with energy saving devices (ESD).

Revised Manuscript Received on October 30, 2019.

* Correspondence Author

Iwan Mustaffa Kamal*, Maritime Engineering Technology Section, Universiti Kuala Lumpur, Malaysian Institute of Marine Engineering Technology, Lumut, Perak, Malaysia.

Md Salim Kamil, Maritime Engineering Technology Section, Universiti Kuala Lumpur, Malaysian Institute of Marine Engineering Technology, Lumut, Perak, Malaysia.

Yaseen Adnan Ahmed, Maritime Engineering Technology Section, Universiti Kuala Lumpur, Malaysian Institute of Marine Engineering Technology, Lumut, Perak, Malaysia.

Nur Aqilah Elias, Maritime Engineering Technology Section, Universiti Kuala Lumpur, Malaysian Institute of Marine Engineering Technology, Lumut, Perak, Malaysia.

© The Authors. Published by Blue Eyes Intelligence Engineering and Sciences Publication (BEIESP). This is an [open access](https://creativecommons.org/licenses/by-nc-nd/4.0/) article under the CC-BY-NC-ND license <http://creativecommons.org/licenses/by-nc-nd/4.0/>.

The major driving force in equipping ships with ESD is the push in getting higher Energy Efficient Design Index (EEDI). The EEDI is issued by the International Maritime Organization (IMO) to promote the use of energy efficient equipment, engines and devices to commercial vessels [1].

There are numerous ESDs that are being used namely Mitsui duct [2], Grothues spoilers [3], Pre-swirl stators [4] etc. According to Carlton [5], ESDs are classified into three zone which are Zone I: Before the propeller, Zone II: At the propeller, and Zone III: Behind the propeller. To date there are not many investigation on the performance of ESD used at Zone III. This ESD that is in the interest in this investigation is known as Post-Swirl Stator. It is believe that the Post-Swirl Stator could suppress the detrimental flow at the aft end of the propeller to improve rudder efficiency. In other words, this post-swirl stator is built as an attempt to deflect the flow from the propeller to turn the propeller's rotational components into useful axial flow.

Min et al. [6] conducted a study using a post-swirl stator which consists of a rudder bulb and a pair of asymmetrical thrust fins being fitted to the left and the right side of the rudder blade. Min et al. [6] has concluded in his study that the slipstream of the propeller produced asymmetrical flow due to the influence of the body of the ship. Due to this asymmetrical flow, the design of the thrust fin must be in asymmetrical shape to enhance thrust. This is shown in his work, where the design of the thrust fin chord and blade span at the right side of the rudder was larger than the the thrust fin attached at the left side of the rudder for a clockwise rotating propeller. It is found that an increase of propulsive efficiency of approximately 6% was obtained when the thrust fin is attached to a position aligned with the shaft centreline. When the thrust fin is attached to a position spaced apart from the shaft centerline in an upward direction by 15% of the propeller radius, the propulsive efficiency is increased at only 4%. Finally when the thrust fin is attached to a position to a position spaced apart from the shaft centerline in an upward direction by 30% of the propeller radius, the propulsive efficiency is increased at only 3%. Finally Min et al. [6] discussed that the he used a thrust fin with a length of 50% of the propeller radius for the left side fin and and 40% for the right side fin without discussing further on the effect of the fin's length to the propulsive efficiency.

Even though there are some reports mentioning that the post-swirl devices as discussed earlier, could improve powering performance of a vessel, there are still a few challenges especially in determining the best configuration and the position of the post-swirl stator.

Therefore, the main purpose of this study is to investigate the best configuration of the post-swirl devices for a typical bulk carrier. In this study a cape-size bulk carrier designed by the National Maritime Research Institute (NMRI) [7], was chosen as the test case.

This bulk carrier is named Japan Bulk Carrier (JBC). The reason for this is there are abundance of measurement data of resistance test, self-propulsion test and PIV measurements of stern field flow field available from NMRI [7].

The assessment of the resistance and the propulsive factors were conducted using CFD simulation. In order to find the optimised design of the ESD, three parameters were laid out and studied. The parameters are the left side fin length, right side fin length and the orientation of the fins. The aim of this study are to improvise the thrust fin design by changing the parameters to get the optimum powering performance result, and to quantify the powering performance of the JBC upon the installation of PSS in model and full scale.

II. THE CONCEPT OF A PSS IN REDUCING DRAG

A PSS is an inclined foil which can be retrofitted to the left and the right side of rudder(s), of a ship at a particular degree and is fixed in its position. At this position, it is able to develop a lift force and a forward thrust from the surrounding flow which directly influences the reduction of trim and the total resistance. The lift force created by the fin surrounded by the incoming flow from the aft bulb and propeller can be decomposed in the x-direction and the z-direction as shown in Figure 1, which is a close-up view of the post-swirl stator retrofitted to the side of a rudder.

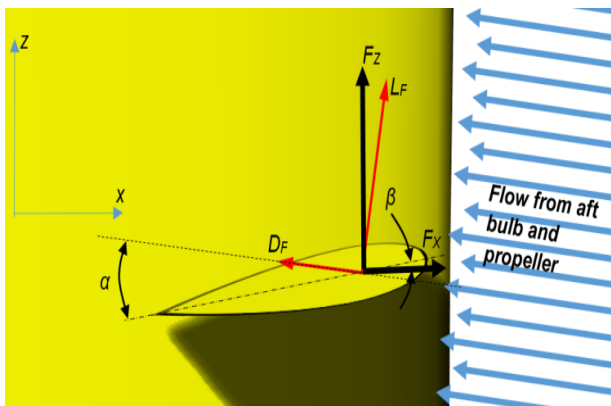


Fig. 1 The PSS fin produces forward thrust force F_X under the stern area at the ship's rudder. The PSS fin also produced lifting force upwards F_Z in correcting the trim of the vessel, thus reducing the total resistance.

The lift force generated by the fin is denoted by L_F , which acts perpendicular to the direction of the incoming water flow from the aft bulb and propeller. Subsequently, the drag force acting on the foil is identified by D_F and is parallel to the direction of the flow. The angle θ , α , and β are defined as the trim angle of the vessel, the angle of attack and the angle of slope of the fin respectively. Therefore the thrust force in the x-direction F_X , generated by the fin can be calculated using Equation (1),

$$F_X = \sin(\alpha + \beta + \theta) \cdot L_F - \cos(\alpha + \beta + \theta) \cdot D_F \quad (1)$$

In cases where the x-component of the force vector is

greater than the drag vector of the same component, there is a reduction of total resistance. Furthermore, the lift generated by the fin, lifts the hull at the aft, thus decreasing the wetted surface area resulting in a reduced frictional resistance. Another feature of this PSS fin as an energy saving device is the ability to correct the vessel's trim. This trim correction due to the force F_Z at z-direction, further reduce the total resistance especially at higher speeds. The force in the z-direction can be calculated using Equation (2),

$$F_Z = \cos(\alpha + \beta + \theta) \cdot L_F - \sin(\alpha + \beta + \theta) \cdot D_F \quad (2)$$

III. THE JAPAN BULK CARRIER

The hull chosen in this investigation is a standard reference hull, the Japan Bulk Carrier (JBC). The JBC hull is a capsize bulk carrier equipped with a stern duct as an energy saving device. In this study only the bare hull of the JBC was used. The JBC hull was designed jointly by NMRI, Yokohama National University and Shipbuilding Research Centre of Japan (SRC) [7]. There are abundance of data available on the towing tank experiments which were conducted at NMRI, SRC and Osaka University. The towing tank experiments include resistance tests, self-propulsion tests and PIV measurements of stern flow fields. There are no full scale ship exists. The main purpose of the development of the JBC hull was for CFD validation puposes in a workshop on CFD in ship hydrodynamics held in Tokyo in 2015. The JBC body plan and the particulars of the hull are illustrated in Figure 1 and Table 1 respectively.

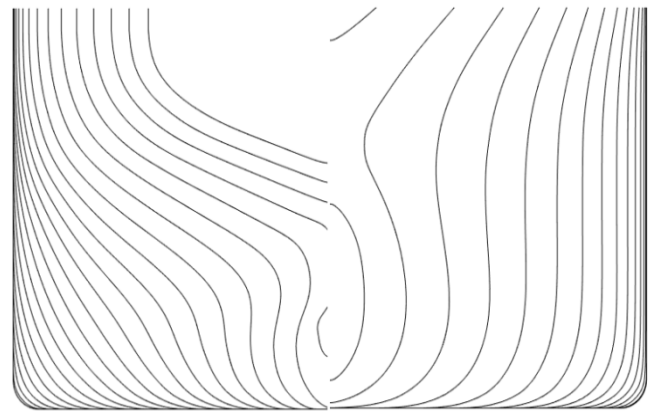


Fig. 2 The JBC body plan with spacing of $L_{pp}/74$ stations. [NMRI]

IV. CFD ASSESSMENT

The investigation was conducted using a commercial CFD code SHIPFLOW 6.3 which is available from FLOWTECH International AB. The solver used in the SHIPFLOW code is a viscous flow RANSE solver XCHAP. XCHAP is a finite volume computation using the Explicit Algebraic Stress Model (EASM) as the turbulence model [8].

A global approach was chosen for the computation where the computational domain was built using the H-O grid topology. All the grids in this study were created using the SHIPFLOW in-house grid generation module XGRID.

The grids generated using XGRID were structured grids with hexahedra cells throughout the whole computational domain.

Table. 1 The main particulars of JBC in model and full scale

Main Particulars		Model scale	Full scale	Units
Length between perpendiculars	L_{PP}	7.0	280.0	m
Length of waterline	L_{WL}	7.125	285.0	m
Max. beam of waterline	B_{WL}	1.125	45.0	m
Draft	T	0.413	16.5	m
Displacement	Δ	2787 kg	182829 tonnes	kg/tonnes
Wetted surface area	S	12.22	19556	m^2
Block coefficient	C_B	0.86	0.86	-
Midship section coefficient	C_M	0.99	0.99	-
LCB (% L_{PP}), fwd+	lcb	2.55	2.55	-
Propeller diameter	D	0.203	8.12	m
Propeller center, long. location (from FP)	x/L_{PP}	0.986	0.986	-
Propeller center, vert. location (below WL)	$-z/L_{PP}$	-0.04	-0.040	-
Propeller rotation	-	CW	CW	-

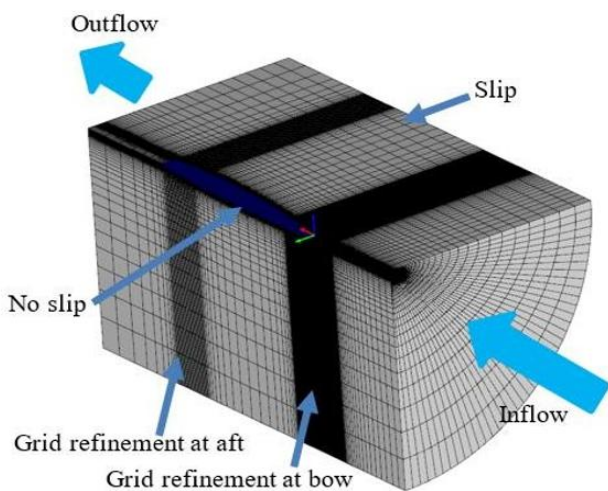


Fig. 3 The computational domain used the H-O grid topology, with the inflow and outflow of the viscous flow computation shown above. No slip condition was applied to the boundary region close to the hull. Note that grid refinements were applied at the bow and the aft region.

A single block grid was used for the JBC hull as proposed by Broberg and Orych [9]. For the PSS fins, a multi-block structured or overlapping grids were used. The viscous flow computations were carried out with the computational domain having six boundaries as shown in Figure 3. The distance between the inlet of the viscous flow and the fore-perpendicular of the ship is at half the length perpendiculars, L_{PP} of the ship. The outlet of the viscous flow is located at 1.5 of length perpendiculars, L_{PP} of the ship behind the aft-perpendicular of the ship. The radius of the

cylindrical outer boundary is at 1.0 length perpendiculars of the ship. This is necessary to prevent from any influence of the blockage effect due to shallow depth of the domain boundary.

A multiple series of computations were carried out under different grid cells size in order to determine the optimal grid cell number. In this grid dependence study, the XGRID command was modified as to control the grid cell distribution. The command ‘*etamax*’ and ‘*zetamax*’ were used in order to increase or decrease the number of planes in circumferential and radial direction respectively. The command of the manual grid control *nu*, *nf*, *nm*, *na* and *nw* were used to increase or decrease the number of cells in the longitudinal direction in the clusters of upstream, forward, midship, aft and wake respectively.

The optimum grid cell that was chosen in the grid dependence study was at approximately 7 million cells. With a CPU of 6 cores processor, the average computation time taken for the simulation to converge is approximately at 40 hours. The computation using Shipflow was done in resistance mode, open-water test mode and the self-propulsion mode in a similar manner in what the author has done in [10]. The propeller was numerically modelled using Lifting Line Theory in Shipflow. The propeller chosen in this study was a five-bladed propeller, the MP687 model available from [7].

V. THE CASE STUDY

The case study using the JBC were set at 27 test cases as illustrated as a parametric space in Figure 4. Each node represents a post-swirl stator with different configuration or parameter. The parameter that were systematically varied in these 27 test cases are (1) right side fin length, (2) left side fin length, and (3) the fin orientation or angle as shown in Figure 5(a), Figure 5(b) and in Table 2. The fin length of the PSS for were quoted as a fraction of the propeller radius. Let say for an example, for a length of 0.3R means that the fin length is 30% of the propeller radius.

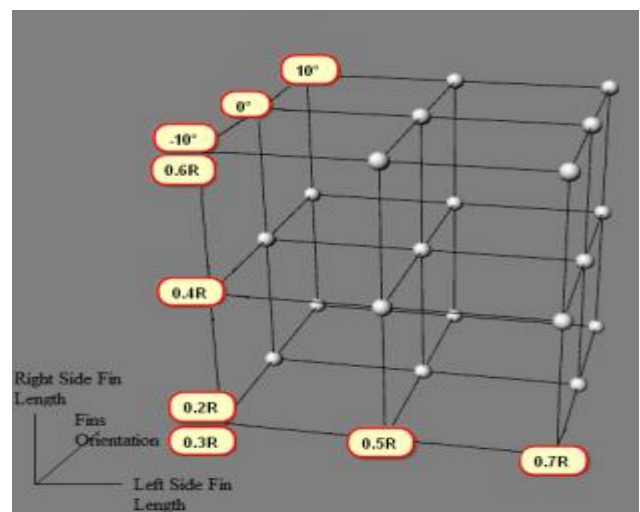


Fig. 4 The 27 test case or case study parametric space of the PSS by varying the right side fin length, the left side fin length, and the fin angle or orientation.

The position of the thrust fins were kept aligned to the shaft centerline in as what have been suggested by Min et al. as discussed earlier in section I. This is the position where the propulsive efficiency is at the highest according to [6]. In the parametric study, the left side thrust fins are set to be longer in terms of its length than the right side thrust fins. The foil profile chosen for both left side and the right side thrust fins was the NACA0012 foil section [11].

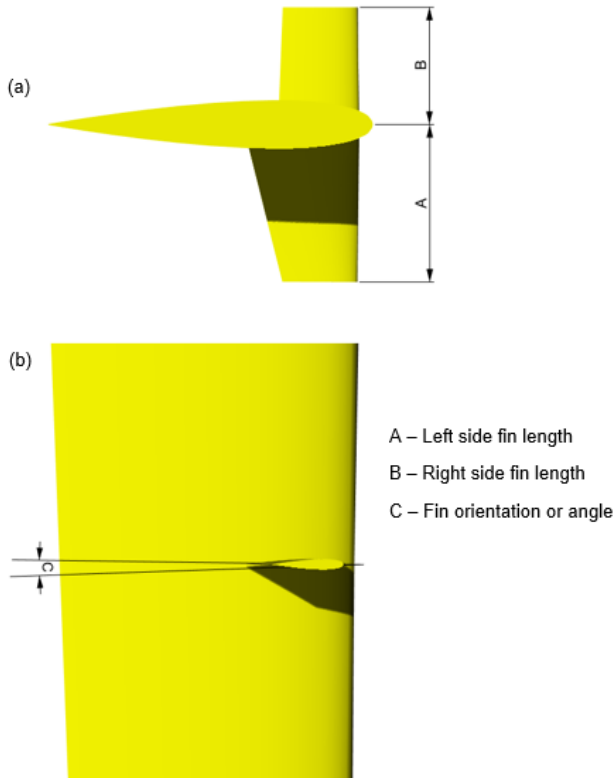


Fig. 5. (a) The top view of a rudder showing the rudder is retrofitted with a right side fin and a left side fin. (b) The side view of the rudder showing the right side fin. The parameters that were varied systematically in 27 different test cases are the left side fin length (A), the right side fin length (B), and the fin angle (C).

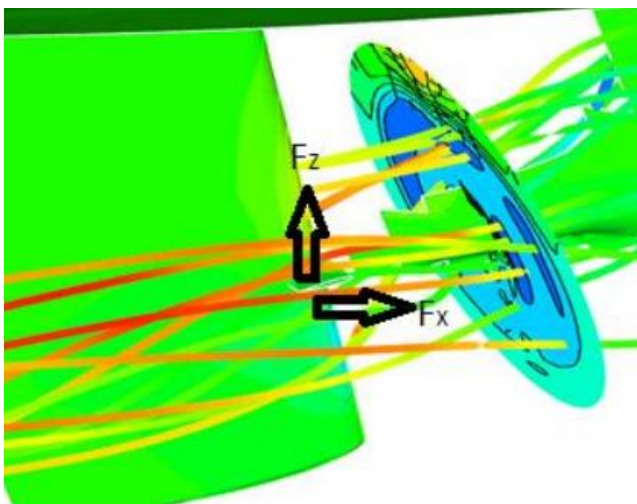


Fig. 6. The simulated streamline through the thrust fins. As stated earlier the drag reduction are from the forward thrust force, F_x and the lift force F_z . The dark color of the streamline tube indicate a higher streamline velocity.

Table. 2 The complete list of the systematically varied parameter i.e. Left side fin length, right side fin length, and fin angle. The length of the fin were quoted as a fraction of the propeller radius.

Case Study #	Left side fin length	Right side fin length	Fin angle (deg)
1	0.3R	0.2R	-10
2	0.3R	0.2R	0
3	0.3R	0.2R	10
4	0.3R	0.4R	-10
5	0.3R	0.4R	0
6	0.3R	0.4R	10
7	0.3R	0.6R	-10
8	0.3R	0.6R	0
9	0.3R	0.6R	10
10	0.5R	0.2R	-10
11	0.5R	0.2R	0
12	0.5R	0.2R	10
13	0.5R	0.4R	-10
14	0.5R	0.4R	0
15	0.5R	0.4R	10
16	0.5R	0.6R	-10
17	0.5R	0.6R	0
18	0.5R	0.6R	10
19	0.7R	0.2R	-10
20	0.7R	0.2R	0
21	0.7R	0.2R	10
22	0.7R	0.4R	-10
23	0.7R	0.4R	0
24	0.7R	0.4R	10
25	0.7R	0.6R	-10
26	0.7R	0.6R	0
27	0.7R	0.6R	10

VI. RESULTS AND DISCUSSION

A. The wake field and the streamline

The streamline of the flow surrounding the aft bulb, the propeller plane and the thrust fins for case study number 20 is shown in Figure 6. It is observed that the velocity of the stream flow at the upper side of the thrust fin is higher than the velocity of the stream flow at the bottom side of the fin, where darker color indicates an increase of velocity. In having a higher velocity at the upper side of the fin and a lower velocity at the bottom side of the fin creates a pressure difference between the pressure at the upper side of the fin and the lower side of the fin. With the lower pressure at the upper side of the fin and a higher pressure at the bottom side of the fin, a lift upwards F_z is created and hence a component of thrust pointing forward F_x is reducing the total resistance of the hull.

The wake field before the post-swirl stator is shown in Figure 7. It is observed that the wake after the propeller is assymetrical. The design of the left-side fin should be longer as illustrated in Figure 7 as to take the advantage of the higher velocity of the slipstream flow in the wake field.

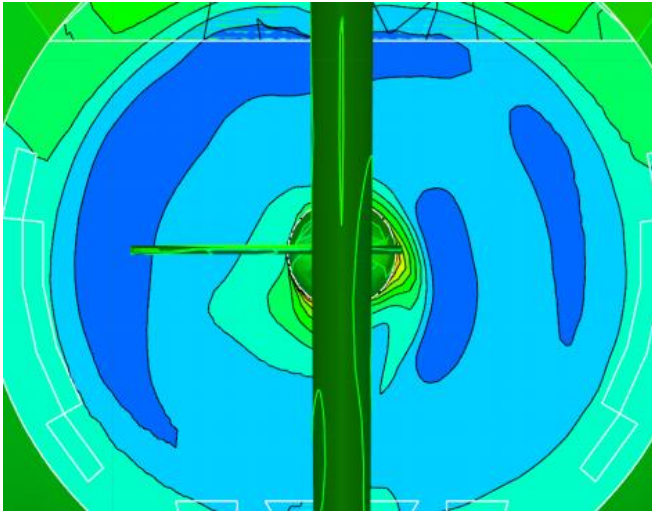


Fig. 7 The wake field before the thrust fins. The thrust fins shown here is with a length of 0.7R for the right side fin and 0.2R for the left side fin.

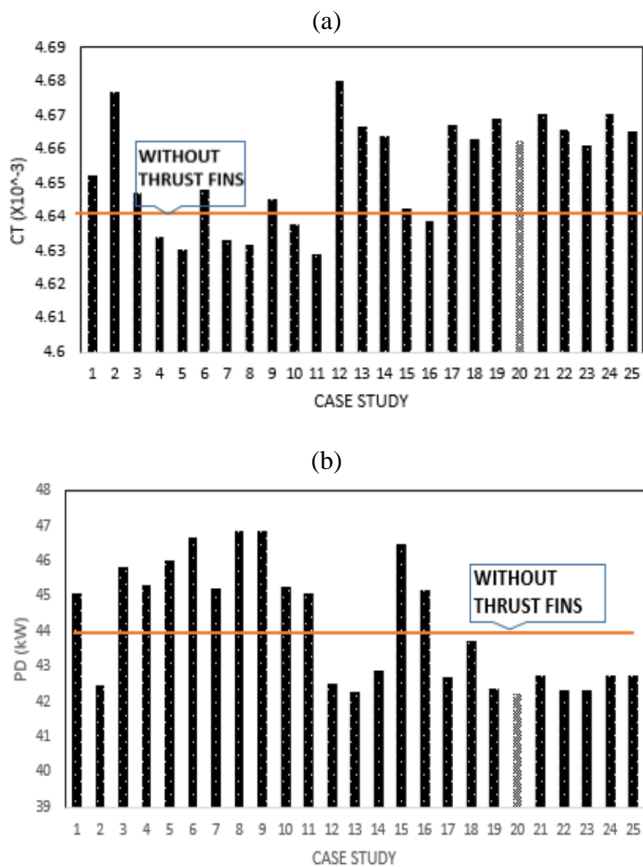


Fig. 8 (a) The plot of the non-dimensional total resistance coefficient with respect to all 25 case studies. **(b)** The plot of the delivered power in watt with respect to all 25 case studies. Note: The horizontal line indicates the value for the JBC bare hull without the post-swirl stator.

B. Total resistance

The result of the total resistance coefficient, C_T is plotted with respect to the case study as shown in Figure 8(a). The total resistance coefficient of the bare hull JBC is at 4.649×10^{-3} . It is observed that there are reductions in the total resistance coefficient for case study 4, 5, 7, 8, 10, 11, and 16. The largest reduction in total resistance coefficient is in case study number 11, where the total resistance coefficient is at

4.629×10^{-3} . The highest total resistance coefficient is in case study number 12, where the total resistance coefficient is at 4.680×10^{-3} .

From this result, we can conclude that by setting the fin angle at 10 degree results in an increase of total resistance. When the fin angle is in between 0 to -10 degree, it seems that less resistance were generated where most of the results shows a reduction in total resistance when the fin angle is set at between 0 to -10 degree. It is clearly understood when we refer back to Figure 1, when the thrust fin angle is at 10 degree, there will be obviously no lift force F_Z generated upwards, and instead the force F_Z will be pushing the hull downwards, thus no trim correction is obtained. Furthermore with this angle of the fin is at 10 degree, there will be no forward thrust F_X produced by the thrust fin, instead a thrust pointing to the stern in the x-direction, which results in an increase of the total resistance.

C. Delivered power

The result of the delivered power, P_D in W is plotted with respect to the case study as shown in Figure 8(b). The delivered power of the bare hull JBC is at 44.91 W. It is observed that there are reduction in the delivered power for case study 2, 12, 13, 14, 17, 18, 19, 20, 21, 22, 23, 24 and 25. The largest reduction in the delivered power is at case study number 20, where the delivered power is at 42.21W. The highest delivered power is at case study number 8, where the delivered power is at 46.87W.

It is observed that there is no correlation between the total resistance and the delivered power, i.e. even though the lowest total resistance is at case study 11, it does not mean that this case study 11 will produce the lowest delivered power when compared to the other case study. The total resistance coefficient of case study no. 20, which is at 4.66×10^{-3} is larger than the bare hull resistance. But due to propeller-hull interaction, the delivered power in case study 20 seems to be the lowest when compared to the other case study. This results proved that with a propeller in action in behind the stern of a vessel, is has a significant impact to the assessment of the performance of a vessel. The assessment which is based only on total drag is not adequate. Any assessment on the powering performance of a vessel should now include the performance test of a vessel in the self-propulsion mode and should not be kept to bare hull resistance test only.

The case study number 20 was finally chosen to be the optimized configuration of thrust fin attached to the rudder of the JBC hull. The configuration of the thrust fins in this case study number 20 consisted of a left side thrust fin at 70% of the propeller radius, a right side thrust fin at 20% of the propeller radius and with fin angle of 0 degree for both fins. However it is still difficult to conclude on any relationship between the length of the fins to the powering performance of the JBC.

Probably we could conclude that, for this specific case, the right side thrust fin should remained at 20% of the propeller radius, the left side thrust fin should be more than the left side fin and the fin angle should remained at 0 degree to achieve the optimum performance.



VII. CONCLUSION

The study on the improvement of powering performance of JBC by adding thrust fins as post-swirl stator was presented. The assessment was made using a viscous flow CFD code using structured grids and hexahedra cells throughout the computational domain. A series of case study were performed with different thrust fins setting or configuration. The configuration were varied in terms of the left side and the right side fin length and the fin angle itself. There are 27 case study with the length varied from 20% to 70% of the propeller radius and from -10 degree to 10 degree of the fin angle. Setting the fin angle at 10 degree results in an increase of total resistance. When the fin angle is in between 0 to -10 degree, it seems that less resistance were generated where most of the results shows a reduction in total resistance when the fin angle is set at between 0 to -10 degree. For this specific case of JBC hull, the right side thrust fin should remained at 20% of the propeller radius, the left side thrust fin should be more than the left side fin and the fin angle should remained at 0 degree to achieve the optimum performance.

REFERENCES

1. IMO, "Guidelines on the method of calculation of the attained Energy Efficiency Index (EEDI) for new ships," *Resolution MEPC. 212 (63)*, Adopted on 2 March 2012, International Maritime Organization, 2012.
2. T. Kitazawa, M. Hikino, T. Fujimoto, and K. Ueda, "Increase in the propulsive efficiency of a ship with the installation of a nozzle immediately forward of the propeller," *Hitachi Zosen Annual Research Report*, 1983.
3. K. Grothues-Spork, "Bilge vortex control devices and their benefits for propulsion," *Int. Shipbuilding Prog.*, 35 (402), 1988.
4. Y.J. Shin, M.C. Kim, W.J. Lee, K.W. Lee, and J.H. Lee, "Numerical and experimental investigation of performance of the asymmetric pre-swirl stator for container ship," *Fourth International Symposium on Marine Propulsor Proceedings*, smp'15, Austin Texas, 2015.
5. J.S. Carlton, *Marine Propellers and Propulsion* (Book style). (3rd Edition), UK: Butterworth-Heinemann, 2012, pp. 321–328.
6. K-S. Min, B-j. Chang, and H-g. Lee, *Thrust fin for ships*. United States Patent, Patent No. US007806067B2, 2010.
7. NMRI. (2015, December). Tokyo 2015, A Workshop on CFD in Ship Hydrodynamics. *JAPAN Bulk Carrier (JBC)*. [Online]. Available: <http://t2015.nmri.go.jp/jbc.html>
8. L. Broberg, B. Regnstrom and M. Ostberg, *XCHAP Theoretical Manual*, FLOWTECH International AB, 2007.
9. L. Broberg and M. Orych, "An efficient numerical technique to simulate the propeller-hull interaction," *International Journal of Innovative Research and Development.*, Vol 1 Issue 10, pp. 494-507, 2012.
10. I. Mustaffa Kamal, M.S. Shamsuddin, and J.R. Binns, "A simplified computational fluid dynamics approach for a self-propelled ship using the actuator disc theory," (Online eBook chapter) *Engineering Applications for New Materials and Technologies*, Springer International Publishing, 2018
11. I.H. Abbott and A.E.V. Doenhoff, *Theory of Wing Sections*, Dover Publications Inc., New York, 1959.

AUTHORS PROFILE



Iwan Mustaffa Kamal is currently a Senior Lecturer and the Head of Marine Design Technology Section (MDT). He received his B.Eng (Hons) in Mechanical Engineering from University of Plymouth, United Kingdom in 1997. He obtained his M.Eng in Marine Technology from Universiti Teknologi Malaysia, Skudai, Johor Bahru in 2009. In 2018, he received his PhD degree in Maritime Engineering (Ship Propulsion) from Australian Maritime College (AMC) at University of Tasmania. He has been working with Universiti Kuala Lumpur Malaysian Institute of Marine Engineering Technology (UniKL MIMET) since March 2006. He is currently an active

member in the Royal Institute of Naval Architect (RINA), Institution of Marine Engineering, Science and Technology (IMarEST) and the Institute of Engineers Malaysia (IEM). He is a registered graduate Mechanical Engineer with the Board of Engineers Malaysia. His research interests are Ship and Propulsion Hydrodynamics, Naval Architecture, and Propeller Design.



Md Salim bin Kamil, graduated with a BSc (Hons) in Naval Architecture and Ocean Engineering from Glasgow University, Scotland, UK; a Master degree in Naval Architecture from University College London (London University), England, UK and a Doctor of Philosophy (Technical Science – Shipbuilding and Ocean Engineering) from Saint Petersburg State Marine Technical University, Saint Petersburg, Russia. He is a registered Professional Engineer with Practising Certificate by the Board of Engineers, Malaysia (Ir, PEng); a registered Chartered Marine Engineer by the Institute of Marine Engineering, Science and Technology, UK (CMarEng); a registered Chartered Engineer by the Engineering Council, UK (CEng). He is also a Fellow member of the Royal Institution of Naval Architects, UK (FRINA), a Fellow member of the Institute of Marine Engineering, Science and Technology, UK (FIMarEST) and a Corporate member of the Institution of Engineers, Malaysia (MIEM).



Yaseen Adnan Ahmed worked as teaching assistant for his supervisor during his postgraduate study. He was awarded with Presidential award from Osaka University Alumni Association for his outstanding result in Master program. After being awarded with doctorate degree, he worked as Research Fellow in International Maritime Research Centre (IMARC), Kobe University, Japan. He also visited Osaka University occasionally as visiting lecturer during his stay in Japan. Later on, he moved to Malaysia after getting the opportunity to work as a senior lecturer in Universiti Kuala-Lumpur, Malaysian Institute of Marine Engineering Technology (UniKL-MIMET). Currently he also acts as a reviewer for well renowned journals. His research interests include Ship Manoeuvring, Intelligent Control, Optimisation, Naval Architecture, Ship Hydrodynamics, CFD and renewable energy.